THE JOURNAL OF PHYSICAL CHEMISTRY B

Article

Water: Two Liquids Divided by a Common Hydrogen Bond

Alan Kenneth Soper

J. Phys. Chem. B, **Just Accepted Manuscript** • DOI: 10.1021/jp2031219 • Publication Date (Web): 25 May 2011

Water: two liquids divided by a common hydrogen bond

Alan K. Soper*

ISIS Department, STFC Rutherford Appleton Laboratory, Harwell Science and Innovation Campus, Didcot, Oxon, OX11 0QX, UK

E-mail: alan.soper@stfc.ac.uk

*To whom correspondence should be addressed

Abstract

The structure of water is the subject of a long and ongoing controversy. Unlike simpler liquids, where atomic interactions are dominated by strong repulsive forces at short distances and weaker attractive (van der Waals) forces at longer distances, giving rise to local atomic co-ordination numbers of order 12, water has pronounced and directional hydrogen bonds which cause the dense liquid close-packed structure to open out into a disordered and dynamic network, with coordination number 4 - 5. Here I show that water structure can be accurately represented as a mixture of two identical, interpenetrating, molecular species separated by common hydrogen bonds. Molecules of one type can form hydrogen bonds with molecules of the other type, but cannot form hydrogen bonds with molecules of the same type. These hydrogen bonds are strong along the bond, but weak with respect to changes in the angle between neighbouring bonds. The observed pressure and temperature dependence of water structure and thermodynamic properties follow naturally from this choice of water model, and it also gives a simple explanation of the enduring claims based on spectroscopic evidence that water is a mixture of two components.

Introduction - mixture models of water and the three-body force

Mixture models have been a recurring theme throughout the history of water research, and have reappeared in different guises right up to the present time.[1] They have been inferred from both structural[2] and spectroscopic[3–7] evidence. The justification for mixture models has sometimes been based on the observation of so-called "isosbestic" behaviour,[2,3] in which a series of spectra as a function of some state parameter such as temperature, pressure or concentration are seen to vary about a common point, suggesting a transfer of population from one type of fluid to another. Other studies have argued that the claim for two-state behaviour in water is not justified on the basis of either spectroscopic[8,9] or diffraction[10] evidence: in both cases continuum computer simulation models of water could be shown to give the same isosbestic behaviour that was used to claim two-state behaviour. More recently x-ray emission spectroscopy on water[7] has been used to claim water

does indeed have two local structures, based on the observation of two peaks in these spectra, one ice-like and therefore assumed to indicate tetrahedral order, and the other gas-like and therefore assumed to indicate hydrogen-bond disordered structure. It has to be said however that a different interpretation of similar data was given in an earlier paper.[11]

Computer simulations of water generally do not show two or more phases as distinct entities since the natural stochastic variations in density and structure, which occur in any disordered system which is undergoing diffusion, are often as large as, over the relevant distance scales, or larger than any supposed fluctuations in density arising from there being two or more components present.[12,13] It is a matter of some irony that at about the same time that Walrafen was stating categorically that the observed temperature dependence of the Raman stretch spectrum of water "provide strong support for the two-state model of water structure",[3] the first computer simulation models of water appeared which naturally gave a continuum view of water interactions.[14,15]

A common feature of many models of the water interaction potential energy is that they do not overtly specify a three-body interaction. Most of the simpler, point charge models of the water interaction potential[16–20] rely on Coulomb repulsion to keep water molecules at their respective positions. In these potentials a negative charge or charges are placed on or near the oxygen atom, while positive charges are placed on or near the hydrogen atoms. Attractive Coulomb interactions between the hydrogen and oxygen atoms on neighbouring water molecules give rise to the hydrogen bonds in these models, while repulsive forces between like-charged oxygen atoms prevent them approaching one another closely unless they are joined by a hydrogen bond. A good example of these forces at work is given in the results from Klein and colleagues.[21] Innumerable refinements and variations of these potentials have occurred, including the use of flexible or polarisable molecules - see for example[22] - but the basic format remains similar.

One notable facet of two-body models of water however is that if the bond angle distribution of the simulated liquid is calculated, that is the distribution of included angles of triplets of water molecules two of which lie at the nearest neighbour hydrogen bond distance from the middle molecule, there is a marked peak at angles $< 60°$,[21,23,24] angles which do not occur even in the

dense form of ice, ice VII, which has a coordination number of 8, and nearly twice the density of hexagonal ice Ih.[25] This suggests there may be a three body term which is missing in these simple models of the water potential.

Recently Molinero and co-workers,[1] have shown that an alternate, effective potential which incorporates a variation of the Stillinger-Weber three-body potential for silicon[26] can be useful for studying many of the underlying features of water properties. In this potential hydrogen atoms do not occur explicitly, but are replaced by a directional three-body potential which depends on the relative separations of triplets of atoms and the included angle between them. This potential appears to give a realistic view of water properties, such as a temperature of maximum density and structure, even if an exact match is not achieved. Using this short ranged three-body potential avoids the need to use long ranged Coulomb potentials to capture water properties.

In fact three-body forces can be incorporated within an effective two-body, pairwise additive framework.[27,28] In that work the structures of elemental tetrahedral glasses such as silicon and germanium are modelled as a mixture of two identical components. The atoms of one component approach those of the other component at the known nearest neighbour distance, but atoms of one component cannot approach other atoms of the same component at this distance. Instead atoms in the same component are constrained to have a near-neighbour distance corresponding to the *second* peak in the radial distribution function. In this way a model of the structure is built up which forces the expected tetrahedrality in these materials. It must be emphasized that the use of two identical but distinct components is a convenient device for generating a three-body body force within a two-body framework but should not be used to claim the two components are distinct states: they have identical structure and are fully interpenetrating.

Notwithstanding all the arguments and counter arguments given above about whether water is a mixture or not, I would like here to apply this method to the structure of water. Two types of otherwise identical water molecules are created labelled 1 and 2. Water molecules of one type can form hydrogen bonds with water molecules of the other type (unlike interactions), but not to water molecules of the same type (like interactions). Instead water molecules of the same type are

weakly held apart to a distance corresponding approximately to the second peak of the oxygen-oxygen radial distribution function for water, namely ∼4.5Å, but there are no other interactions specified at the outset between atoms on like molecules. It is the relative weakness of this like-like interaction coupled with the much stronger hydrogen-bond interaction between unlike molecules that gives this model its essential characteristic. The potentials governing these interactions are put into a NVT Monte Carlo computer simulation of water at 295K and ambient pressure, and the parameters needed to define the interaction potential energies are optimised by comparison of the simulated x-ray and neutron differential scattering cross sections for water with new experimental measurements of the same quantities. This results in a mixture model of water where the two components are identical and fully interpenetrating. The model demonstrates the feature that some neighbours of any given water molecule will be hydrogen bonded to it, while others will not be bonded at all, offering a natural explanation for the enduring claims, based spectroscopic data, that water is a mixture of two components. Changes of temperature or pressure will cause the relative populations of these bonded and non-bonded molecules to change. The simulations show remarkably good agreement with the structural data, and the same interaction potentials can be used to predict the temperature and pressure dependence of both water structure and some thermodynamic quantities, in particular the pressure and specific heat. Intriguingly the results demonstrate a hidden periodicity in water which is closely comparable to that found in hexagonal ice.

Monte Carlo simulation

For the Monte Carlo computer simulation of water at 295K an NVT ensemble of water molecules (500 of each type) is placed in a cubic simulation box of side 31.0516A, giving a number density of 0.0334 molecules/Å^3. Site-site interaction potentials are defined, where specified in terms of a modified Morse potential plus up to 3 additional Gaussian potentials:

$$U(r) = E_0 \left[\exp\left(2\frac{r_0 - r}{w_0(r)}\right) - 2\exp\left(\frac{r_0 - r}{w_0(r)}\right) \right] + \sum_{k=1} E_k \exp\left[-\frac{1}{2}\left(\frac{r_k - r}{w_k}\right)^2 \right] \quad (1)$$

where

$$w_0(r) = \begin{cases} \Delta r_-, & r \leq r_0 \\ \Delta r_+, & r > r_0 \end{cases} \quad (2)$$

and with r_k the position of the minimum (or maximum) of each potential term. The form (2) allows the possibility that the Morse potential decays at a different rate with r beyond the position of the minimum compared to before the minimum. For the present case four sets of such potentials are defined, namely O-O (like), O-O (unlike), O-H (unlike) and H-H (unlike). The potentials for O-H (like) and H-H (like) interactions are set identically to zero. The reason for this particular choice of potential was simply for convenience, since different values of the Morse and Gaussian parameters can give a very wide range of potentials, but this potential form is almost certainly not unique and alternatives could have been considered.

The parameters for these potentials (Table 1) are adjusted in an extended series of trial steps so that the simulation of ambient water at 295K and 0.1MPa has a reasonable pressure ($\sim 0 \pm 100$ MPa) and energy ($\sim -45 \pm 5$kJ/mole), as well as giving an accurate reproduction of new x-ray and neutron diffraction data on heavy and light water and mixtures thereof (see Experimental). The energy value applied is derived from the known heat of vaporisation of water, combined with the likelihood that water molecules in the liquid are more strongly polarised than in the gaseous state.[19] An additional requirement is that when used in a simulation of water at 268K and number density of 0.0381 molecules/Å^3, the simulated pressure is close to the experimental pressure (400 MPa[29]). The use of purely short range potentials, (1), precludes the need to perform long range corrections for the energy and pressure, but otherwise the simulation follows standard procedures.[30] The resulting potential energy functions used in this work, Figure 1, show a strong attraction (deep minimum in the potential energy) for O-H (unlike) interactions, but are primarily repulsive for O-O (unlike) and H-H (unlike) interactions. The O-O (like) interaction has a weak minimum near 4.5Å to encourage the formation of triplets of molecules at the tetrahedral angle, but is otherwise repulsive. The simulations are performed with rigid but disordered molecules as with previous simulations of this kind:[31] these emulate the zero point disorder of the protons and are

an essential prerequisite to obtaining a reasonable fit to the diffraction data, particularly at higher wave vector values.

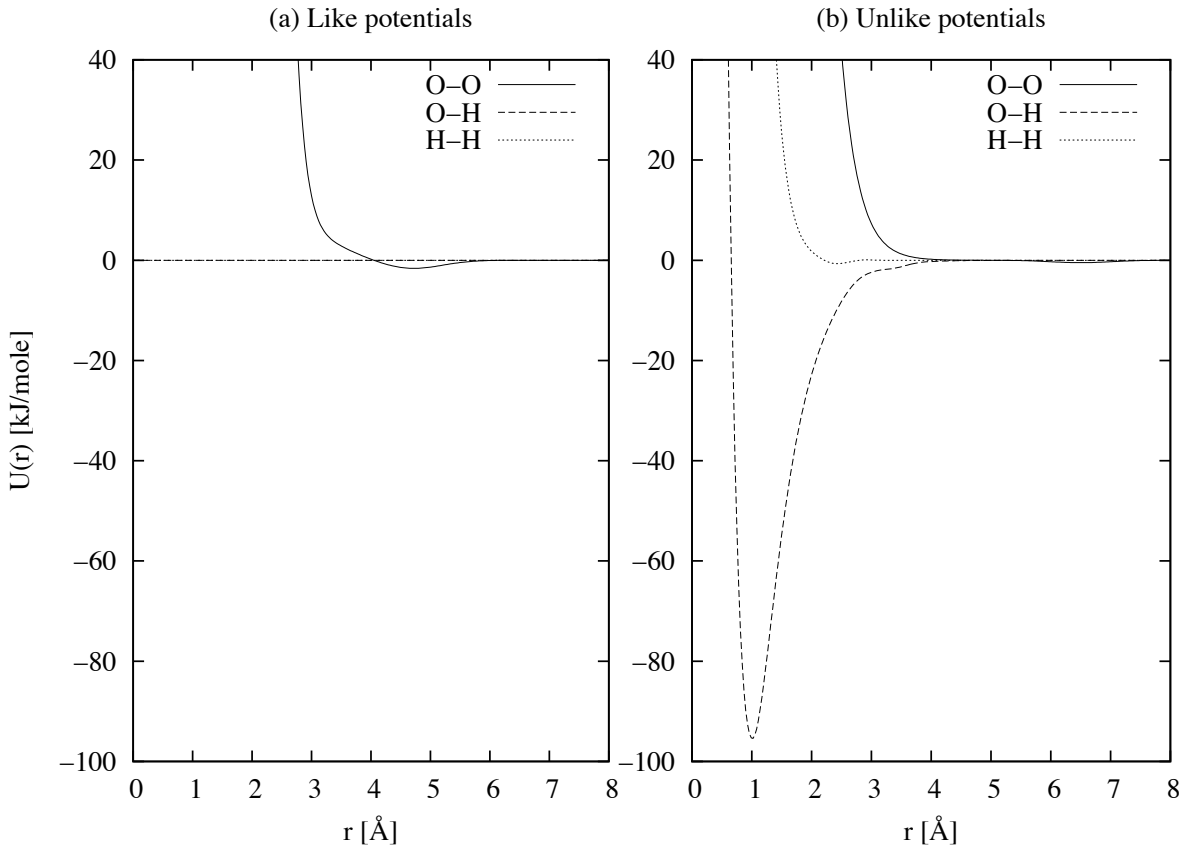

Figure 1: Inter-molecular potentials for like and unlike pairs of molecules. For interactions between molecules of the same type (a) the O-O potential energy has a weak minimum at the position of the *second* minimum of the corresponding radial distribution function. For interactions between molecules of unlike types, the potential energy is dominated by the hydrogen bond between oxygen and hydrogen atoms.

Table 1: List of parameters for the intermolecular potential, equation (1). Energies are given in units of kJ/mole, and distances in Å. It will be noted that there are no prescribed interactions between O-H and H-H on like molecules.

	Atom pair	r_0	Δr_-	Δr_+	E_0	r_1	w_1	E_1	r_2	w_2	E_2	r_3	w_3	E_3
Like	O-O	4.59033	0.34397	0.34397	0.001	3.20	0.50	2.9	4.70	0.5	-1.6	-	-	-
	O-H	-	-	-	-	-	-	-	-	-	-	-	-	-
	H-H	-	-	-	-	-	-	-	-	-	-	-	-	-
Unlike	O-O	5.58163	0.57874	0.57874	0.001	6.50	0.50	-0.5	-	-	-	-	-	-
	O-H	1.00883	0.50876	0.44974	95.15	2.00	0.46	-3.0	2.75	0.2	0.5	3.4	0.2	-0.6
	H-H	3.50063	0.39393	0.39393	0.001	2.38	0.20	-0.9	2.90	0.1	0.1	-	-	-

Experimental

X-ray scattering experiment

X-ray scattering data for water at 295K, ambient pressure, were recorded on a PANalytical x-ray diffractometer, using the white x-ray beam from a silver anode (K_α wavelength = 0.5609Å) using a 2.5mm silica glass thin walled capillary in transmission geometry. A Rh filter was used to eliminate K_β radiation. The scattering data were corrected for background, empty capillary scattering, attenuation, multiple scattering and Compton scattering, and put on an absolute scale of electron units using the Krogh-Moe method.[32] In addition, using diffraction data from silicon crystalline powder as a calibrant, a correction was developed to remove the off-energy scattering that arose from the significant bremsstrahlung radiation in the incident x-ray spectrum. Finally the single atom scattering was subtracted from the diffraction data, which were then normalised to the same single atom scattering to give an x-ray interference differential scattering cross section (Fig. 2(a)), defined by:

$$F_x(Q) = \frac{\sum_{\alpha\beta\geq\alpha}\left(2-\delta_{\alpha\beta}\right)c_\alpha c_\beta f_\alpha(Q) f_\beta(Q) H_{\alpha\beta}(Q)}{\sum_\alpha c_\alpha f_\alpha(Q)^2} \tag{3}$$

where c_α is the atomic fraction and $f_\alpha(Q)$ is the atomic form factor for component α, and the partial structure factor, $H_{\alpha\beta}(Q)$ between atom types α and β is defined as the Fourier transform of the corresponding site-site radial distribution function, $g_{\alpha\beta}(r)$:

$$H_{\alpha\beta}(Q) = 4\pi\rho\int r^2(g_{\alpha\beta}(r)-1)\frac{\sin Qr}{Qr}dr \tag{4}$$

with ρ the atomic number density and Q the wave vector change in the scattering experiment.

Neutron scattering experiment

Neutron scattering gives fundamentally the same information as the x-ray experiment, except that atomic form factors are replaced by numbers - neutron scattering lengths - one for each isotope.

This means that heavy water has a completely different scattering profile compared to normal light water. This can be exploited by measuring heavy and light water, and mixtures thereof, to give direct information on the H-H and O-H correlations in the liquid. In the present instance, as well as the pure liquids, measurements were made on mixtures of 50 mole% and 64 mole% H_2O in D_2O, the latter sample being called "null" in the figures because the net coherent scattering length of hydrogen in this sample is close to zero. Scattering data were corrected for background scattering, container scattering, attenuation, multiple scattering, inelastic scattering, and put on an absolute scale by comparison with the scattering from a known volume of vanadium, which has an almost incoherent scattering cross section. The resulting interference differential scattering cross section (Fig. 2(a)) for neutrons is:

$$F_n(Q) = \sum_{\alpha\beta \geq \alpha} \left(2 - \delta_{\alpha\beta}\right) c_\alpha c_\beta \left\langle b_\alpha \right\rangle \left\langle b_\beta \right\rangle H_{\alpha\beta}(Q) \tag{5}$$

where the angular brackets represent averages over the spin and isotope state of the respective nuclei. The neutron scattering data in this work were recorded as part of the commissioning experiments of the new NIMROD diffractometer at ISIS which is designed for looking at intermediate range structure in liquids, complex fluids, and glasses.[33] Comparison of these datasets with those measured previously on the SANDALS diffractometer at ISIS,[31,34] shows excellent agreement in general, though problems with inelastic scattering from light hydrogen appear to be more pronounced on NIMROD due to the smaller scattered flight path to incident flight path ratio. Work on trying to remove this inelastic scattering more reliably is ongoing.

Results and discussion

Figure 2 (a) and (b) shows the fits to the x-ray and neutron diffraction data at 295K that were achieved in this work while Table 2 gives the densities and temperatures, and calculated mean potential energies and pressures for the all the ambient and non-ambient simulations that were performed in this work. It will be noted from Figure 2(b) that the present model is slightly over-

estimating the height of the first peak in $g_{OO}(r)$: this is in line with other recent x-ray experiments on water[31,35,36] that seem to indicate that the first peak in this function is lower than has traditionally been assumed.

Figure 2(c) shows the simulated O-O, O-H and H-H radial distribution functions separated into their like and unlike counterparts. It can be seen immediately, from the lack of a strong peak in the O-H distribution for like pairs, that there is no hydrogen bonding between like molecules, as expected, but strong hydrogen bonding between unlike pairs. Another feature to emerge in this representation is that the oscillations in $g(r)$, which almost disappear in the total functions, Figure 2(b) beyond $r \approx 8$Å, actually proceed much further than this when separated into like and unlike functions. However they are almost exactly out of phase at longer distances and so cancel each other out in the total function.

Figure 3 shows the distribution of included angles of triplets of oxygen atoms for each of the cases of like-like pairs, unlike-unlike pairs and like-unlike pairs. In all cases two oxygens are considered bonded if their separation is 3.3Å or less. Clearly the like-like and unlike-unlike triplets do not have any peaks below $\theta \approx 90^\circ$ corresponding to the strong repulsion between like atoms below 3Å. However the like-unlike triplets do have quite a marked peak below 60°, so it seems that the presence of this peak in the triplet angle distributions as discussed in the introduction *must* arise from non-bonded molecules in the first coordination shell of water. This will happen even when a deliberate attempt is made, as is done here, to force non-bonded water molecules away from the central molecule. Note however that the coordination number of like oxygen atoms out to the distance used to define a bond, namely $r = 3.3$Å, is only 0.3 atoms whereas that for unlike oxygen atoms at the same distance it is 4.1 atoms, so the occurrence of like-unlike triplets is more than 6 times less likely than for unlike-unlike triplets.

It should also be noted that the O-H coordination number for unlike pairs, integrated out to the first minimum in the unlike O-H $g(r)$, which occurs at $r \approx 2.45$Å is 1.90 hydrogen atoms around oxygen. Including the contributions from H-O as well as O-H interactions would imply the number of hydrogen bonds per water molecule is ≈ 3.8 which is smaller than the unlike O-O coordination

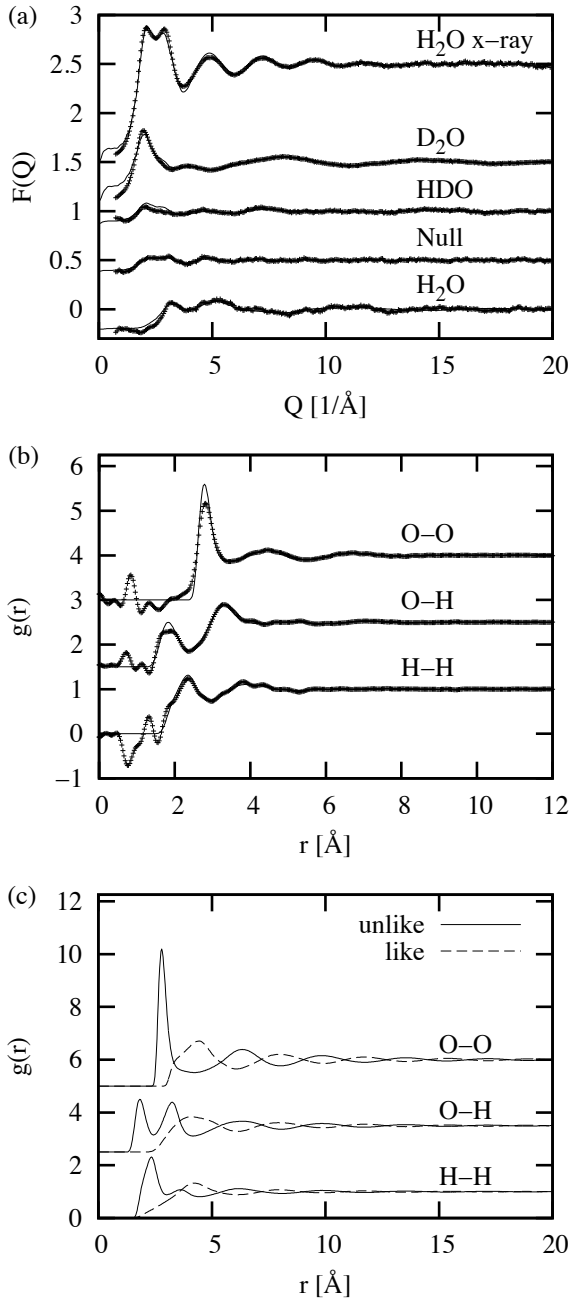

Figure 2: Structure of water using the two component model. (a) Fits (lines) to the x-ray (top) and neutron (lower 4 curves) scattering data (dots) from mixtures of heavy and light water as noted using the intermolecular potentials shown in Fig. 1. (b) Estimated total O-O, O-H and H-H radial distribution functions (rdf) as derived from the simulation (lines) and data (dots). (c) Breakdown of the O-O, O-H and H-H radial distribution functions into their like and unlike counterparts. Graphs (a) and (b) show that simultaneous fits to both x-ray and neutron scattering data can be achieved with the two component model. Graph (c) shows that hydrogen bonding (O-H rdf) is strong between unlike molecules, but non-existent between like molecules, as expected from the definition of the potential. All curves are shifted vertically for clarity.

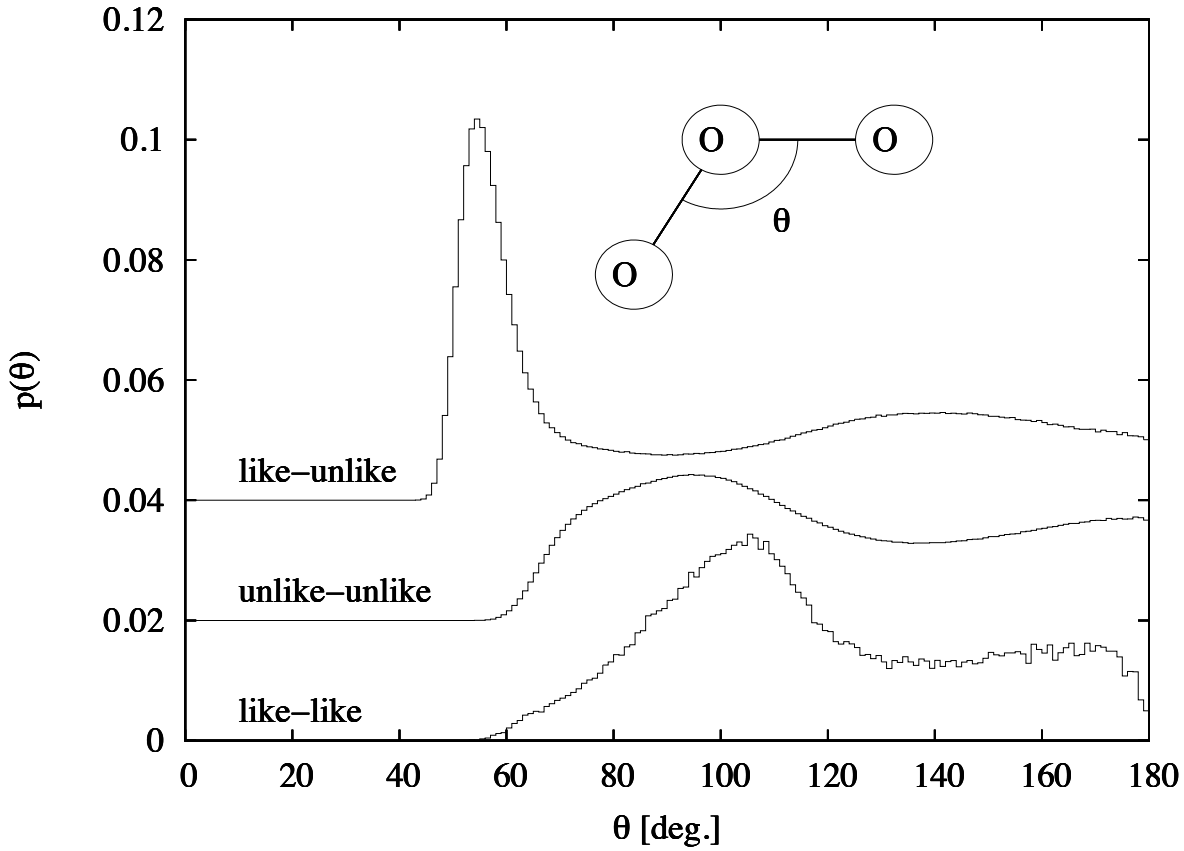

Figure 3: Distribution of included angles for triplets of oxygen atoms. Each triplet is divided into one of three kinds, where the three oxygens are of the same type (like-like), each pair is of the opposite type (unlike-unlike), and where one pair is of the same type and the other of opposite type (like-unlike). The three curves are shifted vertically for clarity.

number of 4.1 quoted above. Hence even in this model there will be some unlike water molecules in the first shall which are not hydrogen bonded to the central molecule.

Table 2: Temperatures, densities, experimental pressures, mean simulated pressures and mean simulated configurational potential energies for water using the two fluid model described in this paper. Pressures are rounded to the nearest 1 MPa (=10 atm.). All simulations are performed in the NVT ensemble, with the quoted energy and pressure values averaged over at least 5000 different simulation boxes. It is found the pressure of the simulations in the temperature range 280-365K increases slightly with increasing temperature, though the variation is not outside the uncertainty in its value.

T [K]	ρ [molecules/Å^3]	Pressure (expt.) [MPa]	Pressure (sim.) [MPa]	Energy (sim.) [kJ/mole]
268	0.03387	27	70	-45.4
268	0.03623	210	313	-46.0
268	0.03807	400	534	-46.8
280	0.03345	0	35	-45.0
288	0.03343	0	62	-44.6
295	0.03338	0	60	-44.1
313	0.03320	0	70	-43.4
343	0.03271	0	89	-41.6
365	0.03225	0	100	-40.4

Table 2 lists the pressures and potential energies that were obtained in the simulations of water using the same potential derived from the ambient data at non-ambient conditions. Moving along the coexistence curve at 0.1MPa there is a slight rise in pressure to near 100MPa at 365K. Note however even at 280K the pressure is 35MPa, so against that baseline the rise is not so significant, in particular when it is realised that the fluctuation of pressure from one simulation box to the next is of order 100MPa. Within this fluctuation the obtained pressures at each pressure and density are remarkably close to their experimental values.

Figure 4 shows the results from these simulations at different temperatures and pressures. Figure 4(a) shows the O-O structure factors as a function of temperature - these can be compared favourably with those shown by Narten *et al*. much earlier.[37] Figure 4(b) shows the corresponding

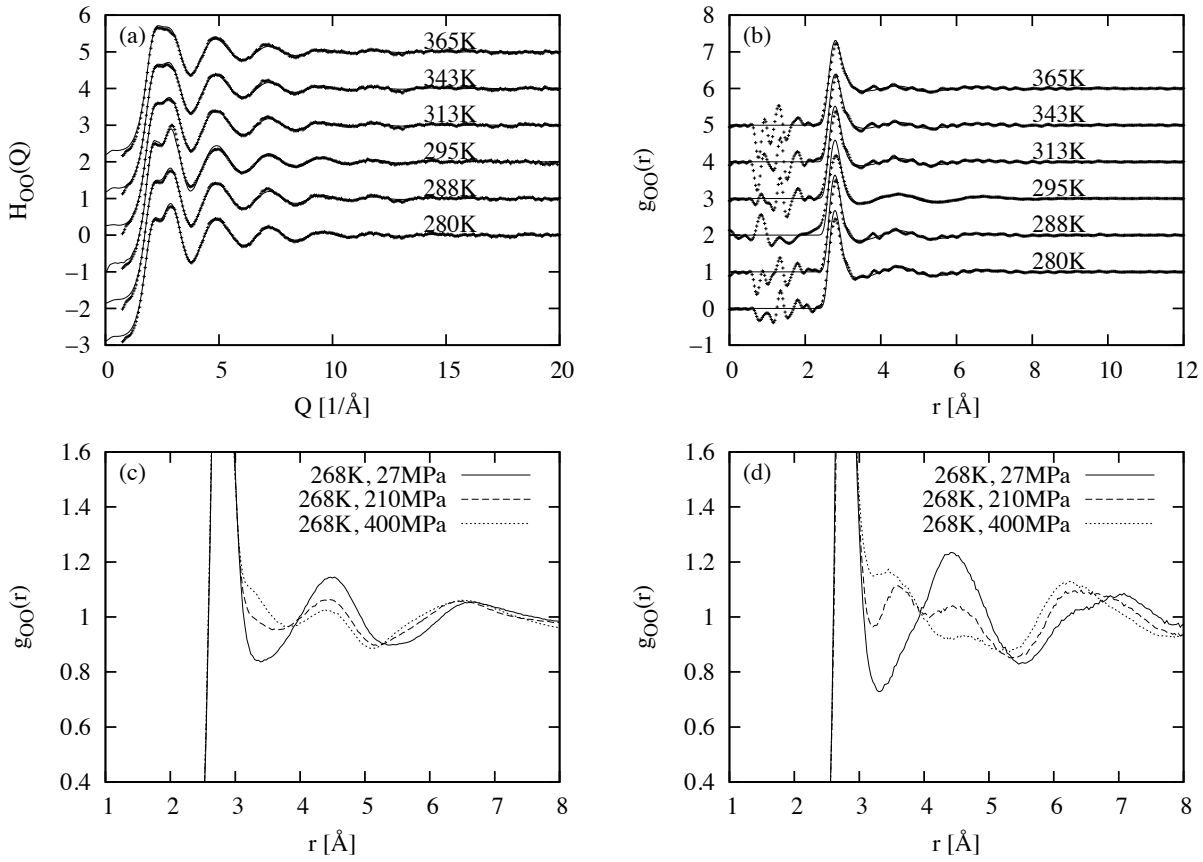

Figure 4: Temperature, (a) and (b), and pressure, (c) and (d), dependence of water structure with the two-fluid model. (a) O-O partial structure factors as a function of temperature for both simulation (lines) and data (dots), equation (4). (b) Corresponding O-O radial distribution functions. (c) Simulated O-O radial distribution function as a function of increased pressure at 268K within the two-fluid model compared to (d) the same functions obtained from the published data,,[29] using a single molecular species. The dots are derived from neutron diffraction data measured at the listed temperatures.

radial distribution functions with the gradual weakening with increased temperature of the main peak and the second peak near 4.5Å. Note that these results were all obtained using the same intermolecular potential energy function that was derived for ambient water.

Figure 4(c) shows the simulated O-O functions with increasing density at 268K, and these curves can be compared to what was estimated directly from the neutron scattering data using a single molecular species (d).[29] Clearly the agreement is not perfect, but the qualitative behaviour of these functions, in which the second peak weakens and extra intensity appears near 3.5Å is closely similar to the experiment.[29,38] In particular the isosbestic points - points where the curves cross over each other - at ∼3.9Å, ∼5.2Å, and ∼6.6Å - are reproduced quite accurately by the two-component model. Bearing in mind that although this is a two component model there is no segregation of the two components, which are identical and fully mixed, it will be seen that isosbestic behaviour is not only a property of mixtures where distinct structural species occur.

Further understanding of how water responds to changes in pressure and temperature is obtained from Figure 5. Here, in (a), is shown the unlike-unlike bond angle distribution as a function of increasing pressure at 268K. The distribution shows a progressive increase in "interstitial" molecules (bond angle $\sim 70°$) as the density increases. These would correspond to the typical angles between unlike-unlike triplets found in higher density forms of ice. In (b) is shown the variation of angle distribution of the O-H vector about the O-O axis between unlike (hydrogen-bonded) molecules. It is seen that the width of these distributions increases gradually with temperature, in a manner that has been observed previously by NMR.[39] The actual standard deviations of these widths are plotted in (c) as a function of temperature and pressure and are found to be somewhat larger than those given by Halle *et al*., but this might be due to the different methods used to extract the bond angle distribution. In particular the NMR study apparently relies on a density functional simulation of water for calibration, and it is well documented that such simulations can give too strong an O-H correlation compared to what is measured experimentally.[40]

Finally Figure 5(d) shows the calculated specific heat for these models. Since the potential is purely pairwise additive this can be calculated in the present case by noting that the total energy of

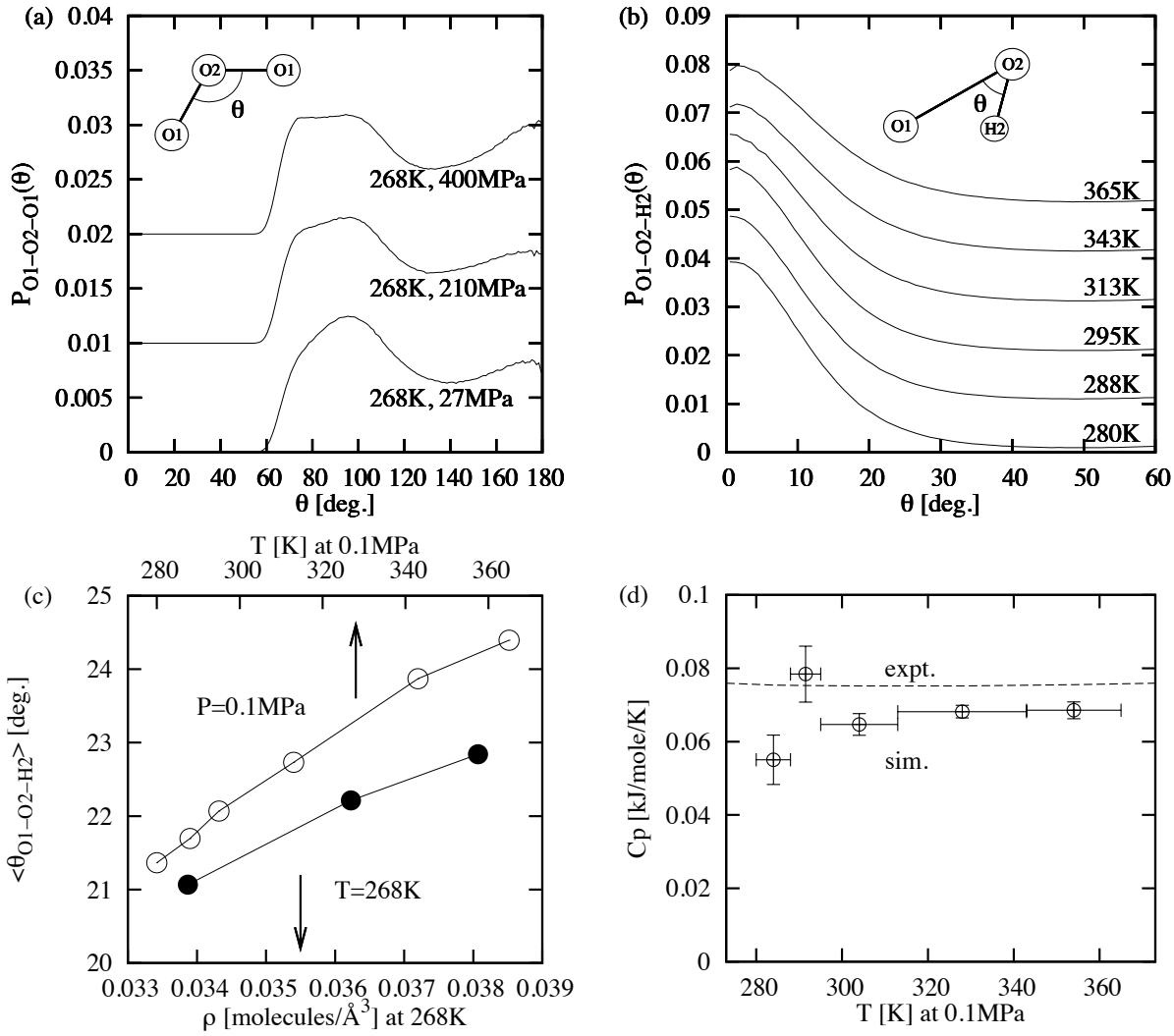

Figure 5: Bond angle distributions and estimated specific heats for the two-fluid model. (a) unlike-unlike bond angle distribution for the two fluid model as a function of increasing density - see Table 2 - at 268K. The distribution shows a progressive increase in "interstitial" molecules (bond angle $\sim 70^\circ$) as the density increases. (b) Bond angle distribution between the O-H vector on one molecule with the O-O vector between unlike pairs of molecules as a function of increasing temperature at a pressure of 0.1MPa. The distributions have been normalised to the $\sin\theta$ distribution that would occur for randomly oriented bonds. (c) Root mean square deviation of the O-O-H bond angle distribution for unlike pairs as a function of density at 268K (lower curve) and as a function of temperature at P=0.1MPa (upper curve). Note how increased temperature and density have a similar effect on this deviation. (d) Simulated specific heat for the two fluid model, from equation 6. The vertical error bars show the fluctuations of this value, based on ~ 5000 molecular configurations, while the horizontal error bars show the temperature range over which each value is averaged. The dashed line shows the experimental values. The error bars become smaller at higher temperatures because the simulated difference is being averaged over a broader range of temperatures.

the system at any state point is the sum of the kinetic and potential energies, and since the pressure remains nearly constant for the simulations at ambient pressure, Table 2, $C_p\left(T \approx \frac{T_1+T_2}{2}\right)$ can be estimated approximately from the expression:[30]

$$C_p(T) \approx \frac{3}{2}R + 2\pi N \sum_{\alpha\beta\geq\alpha} (2-\delta_{\alpha\beta}) c_\alpha c_\beta \int r^2 U_{\alpha\beta}(r) \left[\frac{\left(\rho(T_2) g_{\alpha\beta}^{(T_2)}(r) - \rho(T_1) g_{\alpha\beta}^{(T_1)}(r)\right)}{(T_2 - T_1))}\right] dr \quad (6)$$

where R is the gas constant, $N(=3)$ is the number of atoms per molecule, $\rho(T)$ is the number density and $g_{\alpha\beta}^{(T)}$ is the site-site radial distribution function at temperature T. Once again it is seen that the simulated specific heats are remarkably close to their experimental counterparts, noting that these values have not been fitted when determining the potential parameters. The experimental values have a slight dip near $\sim$310K but the simulated values have too large a variation to be able to see this dip.

It is interesting to discover where this specific heat comes from, so Figure 6 shows the kernal of the integral in (6), $\Delta E_{\alpha\beta}(r) = U_{\alpha\beta}(r)\left(\rho(T_2) g_{\alpha\beta}^{(T_2)}(r) - \rho(T_1) g_{\alpha\beta}^{(T_1)}(r)\right)$ for each of the 6 like and unlike distribution functions in this model. It can be seen that virtually all the contribution comes from a positive term from the OH unlike distribution combined with a negative term from the unlike O-O distribution.[41] Since the O-H potential is strongly negative at the H-bond distance, a positive energy can only arise if bonds have been broken with increasing temperature. The negative contribution from the O-O unlike term arises because, as hydrogen bonds are broken, so the repulsive energy between oxygens which derives from the hydrogen bonding is relaxed. None of the other interactions make a significant contribution to the specific heat. Hence with this model it is seen that a large fraction of the specific heat in water arises directly from the hydrogen bonding, a result which may seem self-evident, but which is important nonetheless.

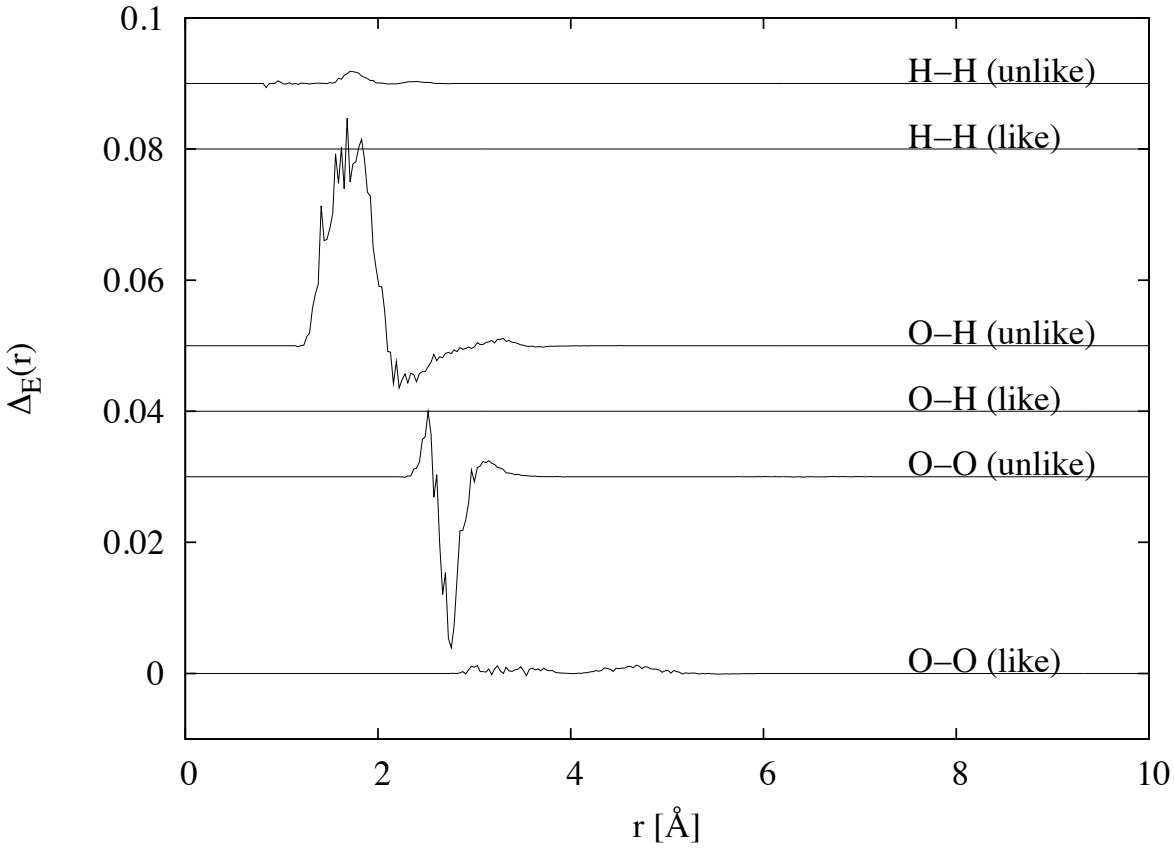

Figure 6: Kernal of the integral in (6) plotted as a function of radius. The difference data are derived from the simulations at 288 and 295K.

Conclusion

The underlying ansatz of the present work is that at any given time a water molecule in the liquid is surrounded by two types of water molecule, those to which it is hydrogen bonded, and those to which it is not bonded. I do not attempt to explain this feature of the model but treat it as fact, although it is worth remembering that standard models of the dense forms of ice include water molecules in the nearest neighbour shell which are not hydrogen-bonded to the central molecule. The two component model that emerges from this assumption is apparently able to capture the structure and thermodynamics of the liquid near ambient conditions surprisingly successfully without resorting to complicated polarisable molecular potentials. Various spectroscopies also strongly hint there are two types of environment around a water molecule in the liquid, bonded and non-bonded,[3,4,7] and these results have been repeatedly used to claim that water is a mixture of two components, one more open and tetrahedral-like, the other more disordered and compressed. Yet serious counter arguments suggest that such spectroscopic results might also be consistent with the traditional continuum models of water that are usually produced by computer simulation methods.[8] The present two component model of water is not a traditional mixture model since the two components have identical structures, are made up of identical molecules, and are fully interpenetrating. What distinguishes the two components is that hydrogen bonds are strong between unlike molecules, but non-existent between like molecules. As a result in this model, bonded and non-bonded water molecules occur quite naturally in the first coordination shell without the need to imagine there are two distinct structural components.

It is important to remember that the two-component model is introduced to generate a three-body force within a two-body framework. The result is that whereas the total density correlation in water damps out very quickly with distance, Figure 2(b), the density correlations associated with like and unlike pairs in the present model proceed to a much longer distance, Figure 2(c). These longer range correlations are hidden in the normal liquid, but one could imagine that if the like correlations are perturbed differently to the unlike correlations, as for example when under pressure or near a hydrophobic surface, a longer range total correlation might appear, such as a

freezing transition. This is of course highly speculative at this stage and has not been investigated in any detail. Strangely enough, for what it is worth, the partial structure factors associated with these like and unlike pairs have opposite sign but equal amplitude peaks in Q space at a Q value ($\approx 1.8\text{Å}^{-1}$) very close to the first peaks in the O-O structure factor of ice Ih, Figure 7, yet there is no peak in the total O-O structure factor of the liquid at this Q value.

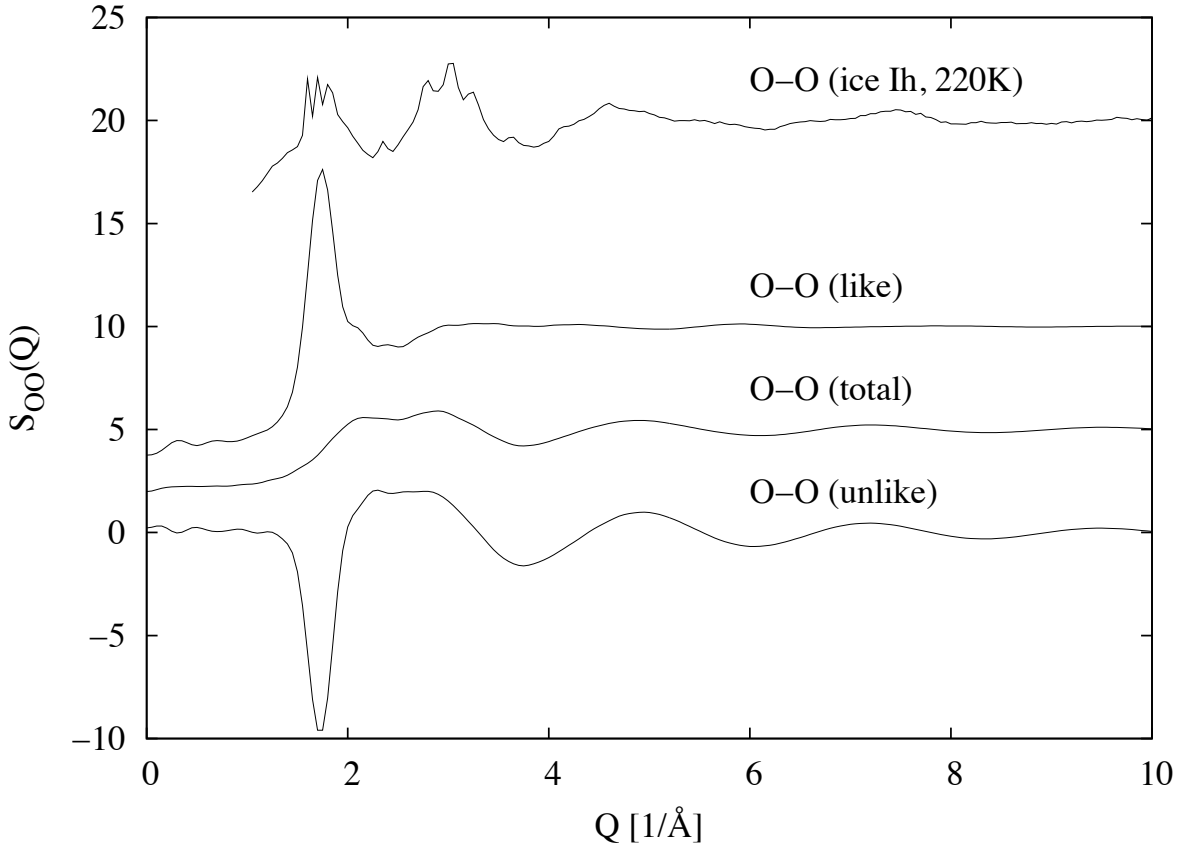

Figure 7: O-O partial structure factors for unlike, total and like pairs for the mixed component model of water. Also shown is the O-O partial structure factor for ice Ih as derived from the data in.[34]

The presence of non-bonded water molecules in the first coordination shell, as exemplified by the presence of a peak below $\theta \approx 60^\circ$ in the like-unlike triplet angle distribution, Figure 3, would presumably be completely prohibited in an ideal ice Ih structure. Hence water structure has to be clearly distinguished from that of ice by the presence of these non-bonded molecules in the first shell.[42] The ideas expressed by the present model therefore appear to fit well with those obtained

in a recent *ab initio* calculation.[43]

Yet another intriguing feature of the model is that when compressed at constant temperature the simulated water has *lower* potential energy than before compression, Table 2. The numbers here are qualitatively consistent with the estimated enthalpy of water under pressure,[44] which if anything would imply an even larger decrease in potential energy with pressure than simulated here. To see how this is, the enthalpy is given in terms of the internal energy and pressure and volume, $\Delta H = \Delta U + \Delta(PV)$. According to[44] the excess enthalpy of water at 273K and 400MPa above ambient pressure is ≈ 2.4kJ/mole. The pressure-volume contribution to the enthalpy change is 6.3kJ/mole, so the net change in potential energy is -3.9kJ/mole. According to Table 2 the change in potential energy in the simulation is -1.4kJ/mole, which is the correct sign even if the wrong magnitude. This might also explain for example why many forms of high density crystalline and amorphous ice can be recovered at ambient pressure: if the temperature is low enough there is insufficient kinetic energy available to allow them to expand up to their (higher potential energy) ambient pressure structures.

Further refinements to this model could be envisaged to improve the fit to both the diffraction and thermodynamic data over a wider range of temperatures and pressures, and it remains to be seen whether this model will have a longer term impact on the overall understanding of water properties.

Acknowledgement

I am indebted to G Johari for help with the thermodynamics of ice phase transitions, for D Bowron for help with setting up the neutron experiments on NIMROD, and E Barney for help with operating the x-ray diffractometer.

Notes and References

(1) Moore, E. B.; Molinero, V. *J Chem. Phys.* **2009**, *130*, Art. No. 244505.

(2) Robinson, G. W.; Cho, C. H.; Urquidi, J. *J. Chem. Phys.* **1999**, *111*, 698–702.

(3) Walrafen, G. *J. Chem. Phys.* **1968**, *48*, 244–&.

(4) Woutersen, S.; Emmerichs, U.; Bakker, H. J. *Science* **1997**, *278*, 658–660.

(5) Rull, F. *Pure Appl. Chem.* **2002**, *74*, 1859–1870.

(6) Wernet, P.; Nordlund, D.; Bergmann, U.; Cavalleri, M.; Odelius, M.; Ogasawara, H.; Naslund, L.; Hirsch, T.; Ojamae, L.; Glatzel, P.; Pettersson, L.; Nilsson, A. *Science* **2004**, *304*, 995–999.

(7) Huang, C. et al. *Proc. Nat. Acad. Sci. USA* **2009**, *106*, 15214–15218.

(8) Geissler, P. *J. Am. Chem. Soc.* **2005**, *127*, 14930–14935.

(9) Smith, J. D.; Cappa, C. D.; Wilson, K. R.; Cohen, R. C.; Geissler, P. L.; Saykally, R. J. *Proc. Nat. Acad. Sci. USA* **2005**, *102*, 14171–14174.

(10) Soper, A. K. *Mol. Phys.* **2008**, *106*, 2053–2076.

(11) Guo, J.-H.; Luo, Y.; Augustsson, A.; Rubensson, J.-E.; Såthe, C.; Ågren, H.; Siegbahn, H.; Nordgren, J. *Phys. Rev. Lett.* **2002**, *89*, 137402.

(12) Clark, G. N. I.; Hura, G. L.; Teixeira, J.; Soper, A. K.; Head-gordon, T. *Proc. Nat. Acad. Sci. U.S.A.* **2010**, *107*, 14003 – 14007.

(13) Soper, A. K. *Pure and Applied Chem.* **2010**, *82*, 1855 – 1867.

(14) Barker, J. A.; Watts, R. O. *Chem. Phys. Lett.* **1969**, *3*, 144–145.

(15) Rahman, A.; Stillinger, F. H. *J. Chem. Phys.* **1971**, *55*, 3336–&.

(16) Bernal, J. D.; Fowler, F. H. *J. Chem. Phys.* **1933**, *1*, 515–548.

(17) Stillinger, F. H.; Rahman, A. *J. Chem. Phys.*' **1974**, *60*, 1545–1557.

(18) Jorgensen, W. L.; Chandrasekhar, J.; Madura, J. D.; Impey, R. W.; Klein, M. L. *J. Chem. Phys.* **1983**, *79*, 926–935.

(19) Berendsen, H. J. C.; Grigera, J. R.; Straatsma, T. P. *J. Phys. Chem.* **1987**, *91*, 6269–6271.

(20) Mahoney, M. W.; Jorgensen, W. L. *J. Chem. Phys.* **2000**, *112*, 8910–8922.

(21) Bagchi, K.; Balasubramanian, S.; Klein, M. L. *J. Chem. Phys.* **1997**, *107*, 8561–8567.

(22) Fanourgakis, G. S.; Xantheas, S. S. *J. Chem. Phys.* **2008**, *128*, Art. No. 074506.

(23) Soper, A. K.; Castner, E. W.; Luzar, A. *Biophys. Chem.* **2003**, *105*, 649–666.

(24) Wikfeldt, K. T.; Leetmaa, M.; Ljungberg, M. P.; Nilsson, A.; Pettersson, L. G. M. *J. Phys. Chem. B* **2009**, *113*, 6246–6255.

(25) Kamb, B.; Davis, B. L. *Proc. Nat. Acad. Sci. U.S.A.* **1964**, *52*, 1433–1439.

(26) Stillinger, F. H.; Weber, T. A. *Phys. Rev. B* **1985**, *31*, 5262–5271.

(27) Soper, A. K. *J. Phys. Condens. Matter* **2007**, *19*, 415108.

(28) Soper, A. K. *J. Phys. Condens. Matter* **2010**, *22*, Art. No. 404210.

(29) Soper, A. K.; Ricci, M. A. *Phys. Rev. Lett.* **2000**, *84*, 2881–2884.

(30) Allen, M. P.; Tildesley, D. J. *Computer Simulation of Liquids*; Oxford University Press, Oxford, 1987.

(31) Soper, A. K. *J. Phys. Condens. Mat.* **2007**, *19*, 335206 (18pp).

(32) Krogh-Moe, J. *Acta Cryst.* **1956**, *9*, 951–953.

(33) Bowron, D. T.; Soper, A. K.; Jones, K.; Ansell, S.; Birch, S.; Norris, J.; Perrott, L.; Riedel, D.; Rhodes, N. J.; Wakefield, S. R.; Botti, A.; Ricci, M. A.; Grazzi, F.; Zoppi, M. *Rev. Sci. Inst.* **2010**, *81*, Art. No. 033905.

(34) Soper, A. *Chem. Phys.* **2000**, *258*, 121–137.

(35) Fu, L.; Bienenstock, A.; Brennan, S. *J. Chem. Phys.* **2009**, *131*, 234702.

(36) Neuefeind, J.; Benmore, C. J.; Weber, J. K. R.; Paschek, D. *Mol. Phys.* **2011**, *109*, 279 – 288.

(37) Narten, A. H.; Levy, H. A. *J Chem. Phys.* **1971**, *55*, 2263–2269.

(38) Okhulkov, A. V.; Demianets, Y. N.; Gorbaty, Y.-E. *J. Chem. Phys.* **1994**, *100*, 1578–1588.

(39) Modig, K.; Pfrommer, B.; Halle, B. *Phys. Rev. Lett.* **2003**, *90*, Art. No. 075502.

(40) Chen, B.; Ivanov, I.; Klein, M.; Parrinello, M. *Phys. Rev. Lett.* **2003**, *91*, Art. No. 215503.

(41) These terms are combined with their statistical weights to produce the final estimate so the magnitudes shown here do not represent the actual contribution to the specific heat.

(42) It should clarified that the term "non-bonded" in this context does not imply the water molecule is not hydrogen bonded to *any* other water molecules. It is simply intended to signify that the molecule is not bonded to the molecule at the centre of the coordinate system.

(43) Chen, W.; Wu, X. F.; Car, R. *Phys. Rev. Lett.* **2010**, *105*, 017802.

(44) Byrne, R.; Thodos, G. *Amer. Inst. Chem. Eng. Journal* **1959**, *5*, 551–555.

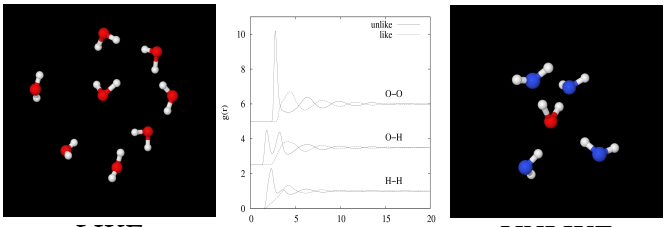

LIKE *UNLIKE*